Inorganica Chimica Acta, 86 (1984) 155–163

Platinum(II) Complexes With Four Ligating Phosphorus Atoms. Crystal and Molecular Structure of $[Pt(PEt_3)_4](ClO_4)_2$. Discussion of Electronic Spectra of Planar and Tetrahedrally Distorted PtP_4 Chromophores

JIŘÍ KOZELKA*, HANS-PETER LÜTHI, ERICH DUBLER

Anorganisch-Chemisches Institut der Universität Zürich, Winterthurerstrasse 190, CH-8057 Zurich, Switzerland

and ROLAND W. KUNZ

Organisch-Chemisches Institut der Universität Zürich, Winterthurerstrasse 190, CH-8057 Zurich, Switzerland

Received November 7, 1983

The crystal and molecular structure of $[Pt(PEt_3)_4](ClO_4)_2$ *has been determined by X-ray diffraction. The compound crystallizes in the orthorhombic space group* P_{bca} *with the cell constants* $a = 26.839(4)$ Å, $b = 13.762(3)$ Å, $c = 19.568(6)$ Å, $z = 8$. *The structure was solved by the heavy-atom-method and refined to a final R-value of 0.053. As a consequence of ligand repulsion the expected square-planar* PtP_4 *coordination exhibits a strong tetrahedral distortion. The* $P–Pt–P_{trans}$ *angles are 150.3° and 150.9°, respectively (instead of 180° for a square-planar structure). The Pt-P bond lengths of 2.33 Å to 2.35 Å are similar to those found in other platinum(II) compounds containing phosphine ligands in* trans*-position.*

Electronic spectra of the cations $[Pt(PR_3)_4]^{2+}$ *(R = Me, Et) have been discussed and compared with those of the related ions* $[Pt(R_2P–CH_2–CH_2–PR_2)_2]^{2+}$*, which have recently [1] been shown to be planar. SCCC-EHMO calculations have been carried out for various geometries of the* PtP_4 *chromophore in order to support the band assignments.*

Introduction

In 1936, Jensen reported an increase in solubility of *cis*-$[PtCl_2(PEt_3)_2]$ in water by adding triethylphosphine in excess [2]. As a consequence of the observed high conductance of the solution he postulated the formation of the ionic species $[Pt(PEt_3)_4]^{2+}$. Recrystallisation lead to the neutral *cis*-complex.

According to Jensen, the solution was colourless. We found, however, that the described procedure always yields a yellow solution. The yellow colour is not compatible with a planar PtP_4 chromophore [1, 3].

Dudell *et al.* [4] investigated the vibrational spectra of $[Pt(PMe_3)_4](NO_3)_2$ and suggested deviations from a planar structure.

We therefore prepared two complexes of the composition $[Pt(PMe_3)_4]Cl_2 \cdot H_2O$ and $[Pt(PEt_3)_4](ClO_4)_2$, respectively. Both compounds exhibit a yellow colour. We report here an X-ray crystal structure analysis of the latter.

Recently, platinum(II) complexes with bidentate phosphine ligands—compounds also containing PtP_4 chromophores—have been synthesized [3]. By an X-ray crystal structure analysis of $[Pt(DEPE)_2](ClO_4)_2$ (DEPE = bis(1,2-diethylphosphino)ethane), a perfectly planar PtP_4 coordination has been found [1]. As the Pt–P bond lengths in this compound do not differ considerably from those in $[Pt(PEt_3)_4](ClO_4)_2$, the rare opportunity was offered to study the influence of the molecular symmetry on the electronic spectra, all other parameters of the chromophore remaining the same. In order to support the spectral assignments, we have carried out EHMO calculations on a number of PtP_4 geometries between D_{4h} and T_d.

Experimental

Preparation of the Complexes

Bis[bis(1,2-dimethylphosphino)ethane]platinum(II)chloride trihydrate ($[Pt(DMPE)_2]Cl_2 \cdot 3H_2O$), bis[bis(1,2-diethylphosphino)ethane]platinum(II)chloride trihydrate ($[Pt(DEPE)_2]Cl_2 \cdot 3H_2O$) and bis[bis(diethylphosphino) ethane] platinum (II) perchlorate ($[Pt(DEPE)_2](ClO_4)_2$) were synthesized as described elsewhere [3, 1].

---

*Present address to which correspondence should be directed: Massachusetts Institute of Technology, Department of Chemistry, Cambridge, MA 02139, U.S.A.

0020-1693/84/$3.00

Tetrakis(trimethylphosphine)platinum(II)chloride Hydrate

Platinum(II)chloride (1 mmol) was stirred with 4.4 mmol of trimethylphosphine and 10 ml of water until all solid was dissolved. The greenish-yellow solution was filtered off and acetone was added to the filtrate. The pink precipitate was filtered off and recrystallized from water/acetone. *Anal.* Calc. for $C_{12}H_{36}Cl_2P_4Pt \cdot H_2O$: C, 24.5; H, 6.5; H_2O, 3.1%. Found: C, 24.5; H, 6.8; H_2O, 3.1%. Above 40 °C, the compound looses 2 equivalents of trimethylphosphine to yield *cis*-$[PtCl_2(PMe_3)_2]$ (the crystal water is lost already at 25 °C).

Tetrakis(triethylphosphine)platinum(II)perchlorate

To a solution of *cis*-$[PtCl_2(PEt_3)_2]$ [2] in ethanol (99.5%) a twofold molar amount of silver perchlorate was added. Silver chloride was filtered off and the solution was treated with an excess of triethylphosphine. Kept standing at room temperature for several hours, this solution yielded yellow crystals of the product. *Anal.* Calc. for $C_{24}H_{60}Cl_2O_8P_4Pt$: C, 33.3; H, 7.0%. Found: C, 33.0; H, 6.8%. Melting point: 164–166 °C.

Suitable single crystals of this compound were obtained from a 0.05 *M* solution of the initial *cis*-complex, using a 5.8-fold molar excess of triethylphosphine. Alternatively, the compound can be recrystallized from hot water.

All starting reactants were supplied by Strem Chemicals, Inc. and used without further purification.

$^{31}P\{^1H\}$ NMR Spectra

^{31}P NMR spectra were taken at ambient temperature from D_2O solutions contained in rotating 10 mm o.d. tubes on a VARIAN XL-200 spectrometer at 81 MHz. In Table I, the δ and $^1J(Pt, P)$ values are compared with data of known PtP_4 complexes. Shifts are relative to external H_3PO_4 85% and are not corrected for susceptibility difference.

The coupling constant $^1J(Pt, P)$ in $[Pt(PEt_3)_4]^{2+}$ is well within the range expected for a platinum(II) compound with phosphine ligands *trans* to each other. The chemical shift is consistent with coordinated triethylphosphine and about 50 ppm high field to the resonance of the DEPE complex. This difference is to be expected for a change from a five-membered chelate ring to the corresponding open system [5].

TABLE I. ^{31}P NMR Data of PtP_4 Complexes (D_2O Solutions).

Compound	δ ^{31}P[ppm]	$^1J(Pt, P)$[Hz]	Ref.
$[Pt(PMe_3)_4]Cl_2$	−20.8	2236	
$[Pt(PMe_3)_4](BF_4)_2$	−21.5	2230	[6]
$[Pt(PEt_3)_4](ClO_4)_2$	4.1	2236	
$[Pt(DMPE)_2]Cl_2$[a]	33.3	2147	[3]
$[Pt(DEPE)_2](ClO_4)_2$[b]	58.5	2121	

[a]DMPE = bis(1,2-dimethylphosphino)ethane. [b]DEPE = bis-(1,2-diethylphosphino)ethane. [c]Positive values indicate low-field shifts.

Crystal Structure Determination

X-ray measurements were carried out on an Enraf-Nonius-CAD4-four-circle-diffractometer. The crystal data and the methods used for intensity collection, structure solution and refinement are summarized in Table II. Preliminary cell parameters were determined from precession and Weissenberg photographs using Mo-Kα radiation. Refined parameters resulted from a least-squares refinement of the orientation angles of 25 reflections centered on the CAD4 diffractometer.

The intensities were corrected for Lorentz and polarisation effects but not for absorption. The programs used for the data reduction and structure analysis were taken from the SDP Nonius program system implemented on a PDP 11/34 computer. The structure was solved by Patterson and Fourier methods and refined to a final residual $R = 0.053$. Hydrogen atoms were not included in the model. In the final cycles Pt, P, Cl and O atoms were refined with anisotropic temperature factors.

The perchlorate oxygen atoms showed very high temperature factors and their coordinates oscillated strongly in subsequent cycles of refinement, most probably a disorder effect, as often observed for perchlorate ions. We therefore fitted the oxygen coordinates, starting with peaks of a difference-fourier map, in the edges of a tetrahedron, with Cl–O distances of 1.42 Å. Then we refined only the temperature factors of the Cl and O atoms, leaving their coordinated fixed.

The final positional and thermal parameters are listed in Table III[†].

Solution Absorption Spectra

The spectra presented in Fig. 3 are photocopies of the original extinction curves which were taken at ambient temperature from H_2O solutions, using 0.1 cm cuvets, on a BECKMAN DK 2A spectrophotometer.

EHMO Calculations

The calculations were performed on an IBM 3033 computer with a local version of an Extended Hückel program. The diagonal elements of the Hückel matrix (H_{ii}) were iterated in self consistent charge and configuration cycles (SCCC), using the quadratic expression $H_{ii}(q) = -(Aq^2 + Bq + C)$ and A, B, C

[†] A list of calculated and observed structure factors is available from the editor on request.

TABLE II. Summary of Crystal Data, Intensity Collection, and Refinement.

Formula	$[Pt(PEt_3)_4](ClO_4)_2$	radiation	Mo-Kα, λ = 0.7107 Å
Mol. wt.	866.64	absortpion coefficient (cm^{-1})	42.8
Dimens. (mm)	0.25 × 0.15 × 0.08	scan method	ω–2θ scan
Cryst. class	orthorhombic	data collected	h ⩾ −1, k ⩾ −1, l ⩾ −1
a (Å)	26.839(4)		2θ ⩽ 40°
b (Å)	13.762(6)	no. of unique reflections	3794
c (Å)	19.568(6)	no. of reflections > 3σ	1610
V ($Å^3$)	7228(5)	no. of observations/no. of variables	8.0
Z	8		
d (calc., g/cm^3)	1.59	structure solution	Patterson and Fourier
d (found, g/cm^3)	1.58	refinement	full-matrix least squares
Systematic absences	0kl: k = 2n + 1	function minimized	$\Sigma w(\lvert F_o\rvert - \lvert F_c\rvert)^2$
	h0l: l = 2n + 1		
	hk0: h = 2n + 1		
Space group	P_{bca}	*w*	$1/\sigma^2(F_o)$
		R	0.053
		R_w	0.088

TABLE III. Positional and Thermal Parameters.[a]

Atom	*x*	*y*	*z*	*B(1, 1)*	*B(2, 2)*	*B(3, 3)*	*B(1, 2)*	*B(1, 3)*	*B(2, 3)*
Pt	0.12732(7)	0.01978(7)	0.23231(6)	0.00098(1)	0.00255(6)	0.00144(3)	−0.0001(1)	0.0001(1)	0.0001(1)
Cl1	0.3672(0)	0.0153(0)	0.0778(0)	0.0023(2)	0.0043(5)	0.0032(2)	−0.0003(6)	−0.0008(5)	−0.0005(9)
Cl2	0.1100(0)	0.5060(0)	0.3927(0)	0.0026(3)	0.0098(10)	0.0023(3)	0.0000(5)	−0.0009(6)	0.0002(12)
P1	0.0724(3)	−0.0303(7)	0.3175(5)	0.0006(2)	0.0040(6)	0.0025(4)	−0.0008(5)	0.0004(4)	−0.0009(9)
P2	0.1861(4)	0.0763(5)	0.3104(6)	0.0010(2)	0.0037(4)	0.0022(3)	0.0000(5)	−0.0006(4)	−0.0004(8)
P3	0.1508(4)	0.1315(8)	0.1473(4)	0.0019(1)	0.0027(7)	0.0014(3)	−0.0002(7)	0.0000(5)	−0.0008(6)
P4	0.1000(5)	−0.0955(7)	0.1534(5)	0.0014(1)	0.0023(7)	0.0018(3)	0.0002(4)	−0.0006(5)	−0.0008(8)
O11	0.3820(0)	0.0635(0)	0.0169(0)	0.0065(11)	0.022(2)	0.0038(9)	0.005(4)	0.005(2)	0.013(4)
O12	0.4092(0)	−0.0300(0)	0.1083(0)	0.0038(7)	0.018(3)	0.0093(23)	0.002(5)	−0.007(2)	−0.000(4)
O13	0.3308(0)	−0.0562(0)	0.0619(0)	0.0082(13)	0.005(2)	0.0214(48)	0.006(4)	−0.011(5)	−0.003(3)
O14	0.3466(0)	0.0839(0)	0.1241(0)	0.0092(15)	0.011(3)	0.0147(27)	0.010(4)	0.013(4)	−0.004(4)
O21	0.0677(0)	0.5500(0)	0.4234(0)	0.0014(7)	0.021(4)	0.0086(19)	−0.001(3)	0.002(2)	−0.012(4)
O22	0.1393(0)	0.4605(0)	0.4439(0)	0.0067(17)	0.009(3)	0.0050(13)	0.000(4)	0.000(3)	0.004(3)
O23	0.1387(0)	0.5781(0)	0.3590(0)	0.0021(10)	0.021(3)	0.0092(17)	−0.001(2)	0.002(2)	0.017(3)
O24	0.0941(0)	0.4353(0)	0.3445(0)	0.0153(29)	0.024(4)	0.0048(16)	−0.011(6)	−0.002(4)	−0.019(3)

Atom	*x*	*y*	*z*	*B, A2*	Atom	*x*	*y*	*z*	*B, A2*
C11	0.0071(0)	−0.037(0)	0.282(0)	3.7(0)	C31	0.1602(17)	0.256(2)	0.187(2)	2.7(6)
C12	−0.0064(0)	0.065(0)	0.252(0)	5.9(0)	C32	0.1042(12)	0.277(2)	0.221(2)	3.3(8)
C13	0.0689(9)	0.073(3)	0.382(2)	2.5(8)	C33	0.0976(14)	0.141(3)	0.086(2)	3.9(8)
C14	0.0260(14)	0.063(2)	0.430(2)	3.6(7)	C34	0.1045(18)	0.221(2)	0.037(2)	7.1(13)
C15	0.0862(0)	−0.148(0)	0.367(0)	5.6(0)	C35	0.2083(12)	0.120(2)	0.095(2)	3.4(7)
C16	0.0348(0)	−0.207(0)	0.389(0)	6.6(0)	C36	0.2324(23)	0.214(2)	0.080(3)	7.6(11)
C21	0.2473(14)	0.083(3)	0.269(2)	3.9(7)	C41	0.1012(15)	−0.218(2)	0.195(2)	2.9(8)
C22	0.2610(17)	−0.012(3)	0.238(2)	6.5(9)	C42	0.1575(17)	−0.243(3)	0.227(3)	5.9(7)
C23	0.1960(14)	−0.016(2)	0.377(2)	2.8(6)	C43	0.1502(16)	−0.109(2)	0.086(2)	2.5(6)
C24	0.2393(20)	0.007(2)	0.427(2)	4.9(10)	C44	0.1433(14)	−0.195(2)	0.037(2)	3.7(10)
C25	0.1829(13)	0.194(3)	0.364(2)	4.1(10)	C45	0.0416(13)	−0.082(3)	0.105(2)	4.6(10)
C26	0.2273(18)	0.257(3)	0.371(2)	6.1(8)	C46	0.0084(20)	−0.178(4)	0.097(3)	7.8(16)

[a] The form of the anisotropic thermal parameter is: exp[−(B(1, 1)*h2 + B(2, 2)*k2 + B(3, 3)*l2 + B(1, 2)*hk + B(1, 3)*hl + B(2, 3)*kl)].

values for P and H due to Basch *et al.* [7]. For Pt, the Pd-values of Munita and Letelier [8] were taken. The off diagonal elements H_{ij} were either calculated by the weighting method of Ammeter *et al.* [9], or, alternatively, according to Ballhausen and Gray [10]. Results reported hereafter are due to the formalism of Ballhausen and Gray, since Ammeter's method lead to unreasonably large mixing of 4s(P)-character into the 5d(Pt) states.

The double zeta STO's of Clementi and Roetti [11] were taken as radial functions for carbon. Hydrogen was represented by a single Slater function with exponent 1.3 and the platinum STO's were taken from the work of Basch and Gray [12]. The virtual phosphorus 4s orbitals were represented by a single Slater function with exponent 1.1 and located at −4 eV (the VSIP-value for 4s(P) estimated from atomic spectra is −4.15 eV [13]).

Discussion of the Crystal Structure

As expected from its stoichiometry, the complex consists of $[Pt(PEt_3)_4]^{2+}$ cations and ClO_4^- anions.

Important interatomic distances and angles are summarized in Table IV–VII. The structure of the cation and the packing diagram are given in Figs. 1 and 2, respectively.

The PtP_4 unit shows quite exactly D_{2d} symmetry. The four Pt–P bond lengths do not deviate significantly from their average value of 2.336 Å; the P–Pt–P(*trans*) angles are 150.4(3) and 150.9(3)°.

The conformations of the methylene C atoms are eclipsed, with C(15), P(1), Pt, P(3), C(35) and C(25), P(2), Pt, P(4), C(45) lying in two vertical planes perpendicular to each other. Since the C–C conformations are very similar for all phosphine ligands (*i.e.*, the three Pt–P–C–C torsion angles are roughly −55, 170, −140° for each ligand), the symmetry of the Pt, P, C skeleton can approximately be described as D_2.

For the 'axial' methylene C atoms C(15), C(25), C(35) and C(45), the Pt–P–C angles are significantly widened, ranging from 119 to 127° (for comparison: in *trans*-$[PtCl_2(PEt_3)_2]$—a complex with a very small ligand repulsion—the Pt–P–C angles range from 97 to 110° [14]), a clear overcrowding effect. As can be seen from the model, there must be considerable repulsion between these 'axial' methylene carbons and the 'equatorial' methylene carbons of the two neighbour ligands. We recognize the cause for the tetrahedral distortion of the planar structure in this repulsion. (The exactly planar ion $[Pt(DEPE)_2]^{2+}$ [1] lacks similar repulsion because of the ethylene bridges!)

The extent of the distortion from a planar configuration found in $[Pt(PEt_3)_4]^{2+}$ is quite rare among four-coordinated second and third row d^8 metal ions. Two very similar examples have already been reported, however: $[Ir(PMePh_2)_4]BF_4$ [15] and $[Rh(PMe_3)_3]Cl$ [16]. The P–M–P angles in these compounds are almost the same as in the present platinum complex. The structures of $[Rh(PMe_3)_4]^+$ and $[Pt(PEt_3)_4]^{2+}$ are nearly coincident—apart from

TABLE IV. Bond Lengths and Bond Angles for $[Pt(PEt_3)_4]^{2+}$.

a) Bond lengths (Å)			
Pt–P(1)	2.329(7)		
Pt–P(2)	2.331(8)		
Pt–P(3)	2.351(7)		
Pt–P(4)	2.332(7)		
P(1)–C(11)	1.885(28)	P(2)–C(21)	1.834(31)
P(1)–C(13)	1.896(26)	P(2)–C(23)	1.842(27)
P(1)–C(15)	1.925(34)	P(2)–C(25)	1.925(29)
P(3)–C(31)	1.892(26)	P(4)–C(41)	1.863(26)
P(3)–C(33)	1.870(3)	P(4)–C(43)	1.893(26)
P(3)–C(35)	1.863(29)	P(4)–C(45)	1.843(31)
C(11)–C(12)	1.572(46)	C(21)–C(22)	1.493(47)
C(13)–C(14)	1.495(37)	C(23)–C(24)	1.548(39)
C(15)–C(16)	1.656(47)	C(25)–C(26)	1.481(40)
C(31)–C(32)	1.668(36)	C(41)–C(42)	1.675(40)
C(33)–C(34)	1.477(42)	C(43)–C(44)	1.542(37)
C(35)–C(36)	1.476(44)	C(45)–C(46)	1.595(49)
b) Selected bond angles (°)			
P(1)–Pt–P(2)	93.35(27)	P(2)–Pt–P(3)	93.67(27)
P(1)–Pt–P(3)	150.35(29)	P(2)–Pt–P(4)	150.93(28)
P(1)–Pt–P(4)	94.22(28)	P(3)–Pt–P(4)	93.48(25)
Pt–P(1)–C(11)	110.0(9)	Pt–P(2)–C(21)	109.5(11)
Pt–P(1)–C(13)	106.6(9)	Pt–P(2)–C(23)	109.4(9)
Pt–P(1)–C(15)	119.3(10)	Pt–P(2)–C(25)	127.2(10)
Pt–P(3)–C(31)	109.7(8)	Pt–P(4)–C(41)	108.7(9)
Pt–P(3)–C(33)	107.2(10)	Pt–P(4)–C(43)	107.8(8)
Pt–P(3)–C(35)	124.0(9)	Pt–P(4)–C(45)	122.8(11)
C(11)–P(1)–C(13)	103.5(12)	C(21)–P(2)–C(23)	102.7(13)
C(11)–P(1)–C(15)	108.8(14)	C(21)–P(2)–C(25)	103.8(14)
C(13)–P(1)–C(15)	107.4(14)	C(23)–P(2)–C(25)	101.5(13)
C(31)–P(3)–C(33)	107.5(13)	C(41)–P(4)–C(43)	101.4(12)
C(31)–P(3)–C(35)	101.0(13)	C(41)–P(4)–C(45)	109.2(14)
C(33)–P(3)–C(35)	106.4(13)	C(43)–P(4)–C(45)	104.8(13)

TABLE V. Best Least-Squares Plane for $[Pt(PEt_3)_4]^{2+}$.

Atoms defining mean plane	Displacement from mean plane (Å)	Equation of mean plane
Pt	0.0	Ax + By + Cz − D = 0
P(1)	−0.599	A = 0.7205
P(2)	0.585	B = −0.6934
P(3)	−0.599	C = −0.0084
P(4)	0.585	C = 2.2352

TABLE VI. Selected Dihedral Angles (°).

Atoms defining plane 1	Atoms defining plane 2	Dihedral angle
Pt, P(1), P(3)	Pt, P(2), P(4)	90
Pt, P(1), P(2)	Pt, P(3), P(4)	139
Pt, P(2), P(3)	Pt, P(1), P(4)	139

TABLE VII. Torsion Angles (°).

Pt–P(1)–C(11)–C(12)	–56	Pt–P(2)–C(21)–C(22)	–54
Pt–P(1)–C(13)–C(14)	165	Pt–P(2)–C(23)–C(24)	172
Pt–P(1)–C(15)–C(16)	–146	Pt–P(2)–C(25)–C(26)	–136
Pt–P(3)–C(31)–C(32)	–59	Pt–P(4)–C(41)–C(42)	–55
Pt–P(3)–C(33)–C(34)	170	Pt–P(4)–C(43)–C(44)	170
Pt–P(3)–C(35)–C(36)	–143	Pt–P(4)–C(45)–C(46)	–139
P(1)–Pt–P(2)–C(21)	159	P(1)–Pt–P(3)–C(31)	60
P(1)–Pt–P(2)–C(23)	47	P(1)–Pt–P(3)–C(33)	–57
P(1)–Pt–P(2)–C(25)	–75	P(1)–Pt–P(3)–C(35)	179
P(1)–Pt–P(4)–C(41)	–51	P(2)–Pt–P(1)–C(11)	157
P(1)–Pt–P(4)–C(43)	–161	P(2)–Pt–P(1)–C(13)	46
P(1)–Pt–P(4)–C(45)	78	P(2)–Pt–P(1)–C(15)	–76
P(2)–Pt–P(3)–C(31)	–44	P(2)–Pt–P(4)–C(41)	53
P(2)–Pt–P(3)–C(33)	–160	P(2)–Pt–P(4)–C(43)	–56
P(2)–Pt–P(3)–C(35)	76	P(2)–Pt–P(4)–C(45)	–178
P(3)–Pt–P(1)–C(11)	54	P(3)–Pt–P(2)–C(21)	–50
P(3)–Pt–P(1)–C(13)	–58	P(3)–Pt–P(2)–C(23)	–162
P(3)–Pt–P(1)–C(15)	–179	P(3)–Pt–P(2)–C(25)	76
P(3)–Pt–P(4)–C(41)	157	P(4)–Pt–P(1)–C(11)	–51
P(3)–Pt–P(4)–C(43)	48	P(4)–Pt–P(1)–C(13)	–162
P(3)–Pt–P(4)–C(45)	–74	P(4)–Pt–P(1)–C(15)	76
P(4)–Pt–P(2)–C(21)	54	P(4)–Pt–P(3)–C(31)	165
P(4)–Pt–P(2)–C(23)	–58	P(4)–Pt–P(3)–C(33)	48
P(4)–Pt–P(2)–C(25)	–180	P(4)–Pt–P(3)–C(35)	–76

the end-of-chain methyl groups of the latter, of course. Apparently, steric effects alone are determining the deviations from the square planar coordination in these ions.

Therefore, the cation $[Pt(PMe_3)_4]^{2+}$, as well as related palladium complexes, $[Pd(PR_3)_4]^{2+}$, which have not been synthesized up to date, are expected to have roughly the same structure as $[Pt(PEt_3)_4]^{2+}$ and $[Rh(PMe_3)_4]^+$.

EHMO Calculations and Spectral Assignment

As the resolution of the absorption spectra of the tetrahedrally distorted chromophores is somewhat worse than that of the planar ones, only two bands can be correlated with their planar counterparts, namely the bands 'A' and 'B' (Fig. 3).

In a previous work on planar PtP_4 chromophores [3], band 'A' has been assigned to a Rydberg transition from a 5d platinum orbital to a linear combination of 4s phosphorus orbitals. However, an alternative assignment to a platinum-internal d–p transition could not be excluded. For band 'B', two assignments have been discussed: i) to the ligand-to-metal charge transfer ($4e \rightarrow 4b_2$) ii) to a Rydberg transition within the ligand system (*i.e.*, ($4e \rightarrow 5a_1$) or ($3b_2 \rightarrow 6e$))*.

It was our aim to investigate whether the band shifts observed upon tetrahedral distortion of the chromophore could serve as a clue for a more definitive assignment.

The EHMO calculations were performed on a hypothetical $[Pt(PH_3)_4]^{2+}$ species. A test calculation on the $[Pt(PMe_3)_4]^{2+}$ cation showed no significant changes in both, eigenvalues and MO-coefficients.

Starting from a planar PtP_4 geometry and PH_3 conformations as given in Fig. 4**, the two P–Pt–P angles were bent simultanously by 2α within vertical planes (*i.e.*, $\alpha = 15°$ corresponds to $P\text{–}Pt\text{–}P_{trans}$ angles of 150°; for $\alpha = 35°$, the PtP_4 unit is roughly tetrahedral). In this manner, the symmetry of the species remains D_{2d}.

For Pt–P bond lengths the average of the distances found in $[Pt(PEt_3)_4](ClO_4)_2$ and $[Pt(DEPE)_2](ClO_4)_2$ [1], 2.32 Å, was taken. P–H bond lengths of 1.447 Å and H–P–H angles of 105° were assumed§.

While the EHMO model is not very suitable for predicting absolute energy values, it is expected to properly indicate band shifts and intensity changes for related chromophores.

In Fig. 5a, calculated one-electron energies of the highest occupied and the lowest unoccupied molecular orbitals are plotted *versus* α. Obviously, for $4b_2$, a pronounced energy lowering with increasing α is predicted. This is not surprising, as the overlap of ligand σ orbitals with $5d_{xy}(Pt)$ (remember the coordinate system taken for D_{2d}!) becomes smaller. Thus, ligand-field bands are expected to be shifted to lower energies. In fact, the broad shape of bands observed in the low-energy part or the spectra of $[Pt(PR_3)_4]X_2$ could be due to a superposition of the Rydberg bands with the red-shifted ligand-field bands. As the low-energy absorption penetrates the visible region, the compounds are yellow.

---

*The irreducible representations correspond to d_{2d}.

**Changes in the PH_3 conformations have shown not to affect the results significantly.

§In free phosphine, P–H bond lengths of 1.42 Å and H–P–H angles of 93.3° have been found [17]. In complexes, lengthening of the bonds and widening of the angles are expected.

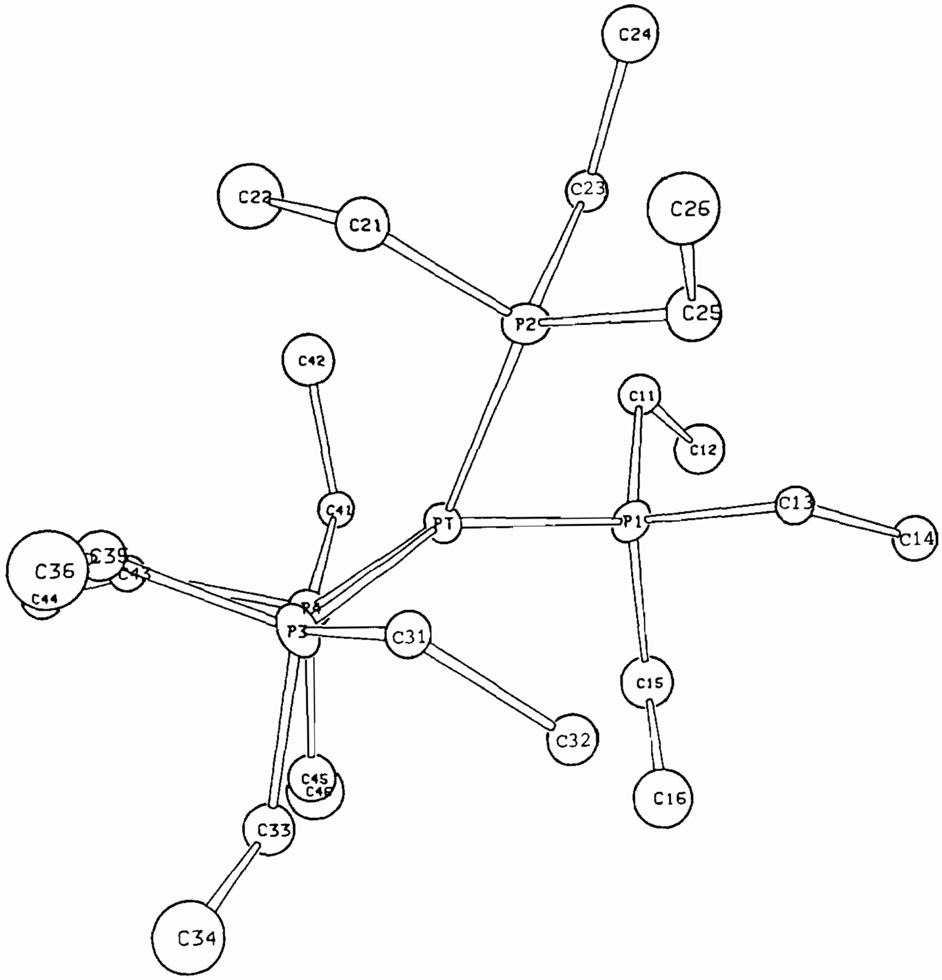

Fig. 1. An ORTEP picture of the cation $[Pt(PEt_3)_4]^{2+}$ (hydrogen atoms not included).

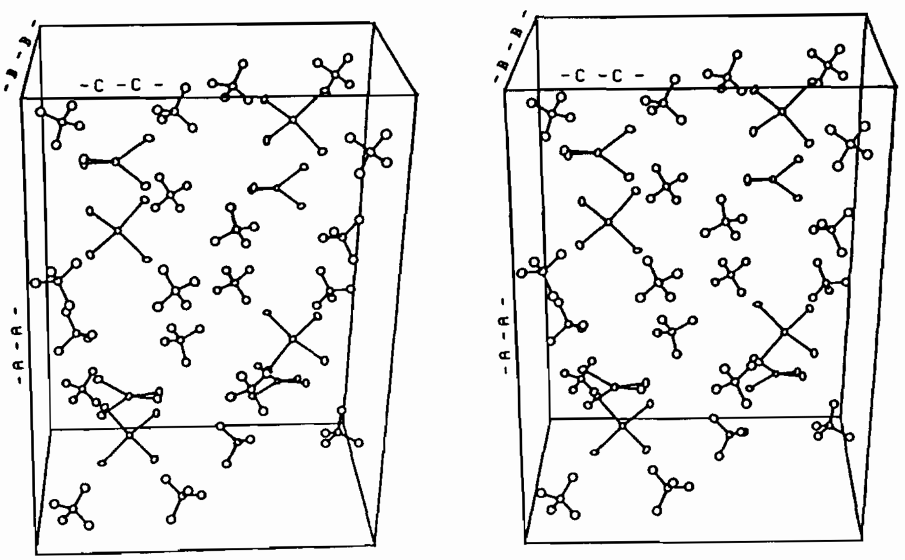

Fig. 2. Stereoview of the crystal packing of $[Pt(PEt_3)_4](ClO_4)_2$. Only the PtP_4 (longer bonds) and ClO_4 (shorter bonds) units have been depicted, for clarity.

The energy of $5b_2$ (= preponderantly $6p_z$(Pt)) is shown to increase with increasing α. However, this behaviour can be inverted by fitting slightly different H_{ii} values or by using alternative approximating formulas for the H_{ij}'s. Hence, for 'A', which is only slightly red-shifted in the tetrahedrally distorted ions (Fig. 3), one cannot decide whether the acceptor orbital is $5b_2$ or 6e, regarding the calculated orbital energies alone.

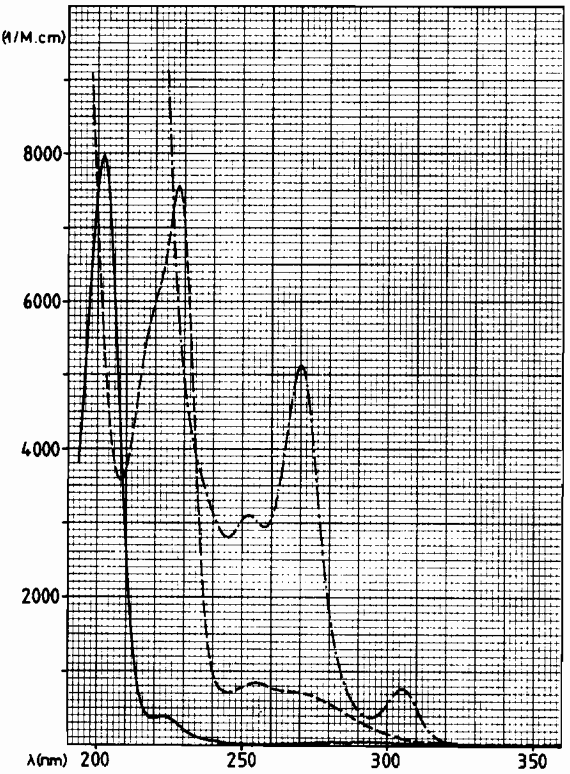

Fig. 3. Solution absorption spectra of [Pt(DEPE)$_2$](ClO$_4$)$_2$ (——) and [Pt(PEt$_3$)$_4$](ClO$_4$)$_2$ (- - -).

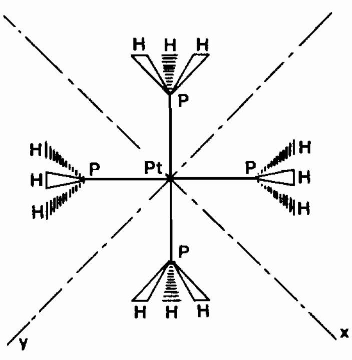

Fig. 4. Coordinate system of the [Pt(PH$_3$)$_4$]$^{2+}$ ion used in the EHMO calculations.

Band 'B' experiences a red shift of *ca.* 3500 cm^{-1} in the spectra of the tetrahedrally distorted complexes, which is something between the red shift expected for $4e \rightarrow 4b_2$ (~7000 cm^{-1}) and the constancy of transition energy predicted for ($4e \rightarrow 5a_1$). The transition ($3b_2 \rightarrow 6e$) can be excluded because its intensity should drop significantly in the distorted chromophore (see Table VIII).

Let us compare the intensities of 'A' and 'B' with each other (Table VIII). In the case of the planar chromophore, the calculated oscillator strength for band 'B' is either 0.578 or 0.459, dependent on whether we assign it to ($4e \rightarrow 4b_2$) or to ($4e \rightarrow 5a_1$). The observed intensity ratio for the two bands (Fig. 3) is roughly 'A':'B' = 1:10. Hence, 'A' is not likely to be due to an allowed d–p transition (*i.e.*, ($5e \rightarrow 5b_2$) or ($4a_1 \rightarrow 5b_2$)), as for these, the calculated oscillator strengths are of a similar order of magnitude as those for 'B', *i.e.*, 0.267 and 0.352, respectively. For the transitions to 6e, considerably lower intensities are predicted. The oscillator strength of 0.065 calculated for ($2b_1 \rightarrow 6e$) seems to be in a reasonable agreement with the intensity observed for 'A'. The same result is obtained by comparing calculated osc. strengths for the tetrahedrally distorted species.

Accordingly, the probable acceptor orbital for the transition 'A' is 6e (composed predominantly of 4s(P)), as suggested by Kozelka and Ludwig [3].

As an additional proof, we investigated the influence of the 4s(P) orbitals on the electronic structure and hence on the MO diagrams. In Fig. 5(b), results of an analogous series of calculations, in which 4s(P) orbitals were not included, are displayed. Obviously, no acceptable assignment for band 'A' can be given based on this variant of calculation. For transitions from 5d(Pt) to $4b_2$, a strong red shift, accompanied by a pronounced intensity drop, is expected, when α increases (the character of $4b_2$ changes from preponderant $6p_z$ to preponderant $5d_{xy}$*). On the other hand, a large blue shift is predicted for 5d excitations to $5b_2$ by these calculations. Neither of the two behaviours is observed for band 'A'. Hence, the 4s phosphorus orbitals, often omitted, must be included in MO calculations and spectral assignments.

Table IX summarizes the spectral data of [Pt(PEt$_3$)$_4$](ClO$_4$)$_2$ and [Pt(PMe$_3$)$_4$]Cl$_2$. For comparisons with the planar PtP$_4$ chromophores, see Table IV of Ref. 3.

Acknowledgement

We thank Mr. N. Seferiadis for recording the precession and Weissenberg photographs.

---

*Calculations of oscillator strengths indicate an intensity drop of 55% for ($4a_1 \rightarrow 4b_2$) and 85% for ($5e \rightarrow 4b_2$). The transition ($2b_1 \rightarrow 4b_2$) is symmetry-forbidden.

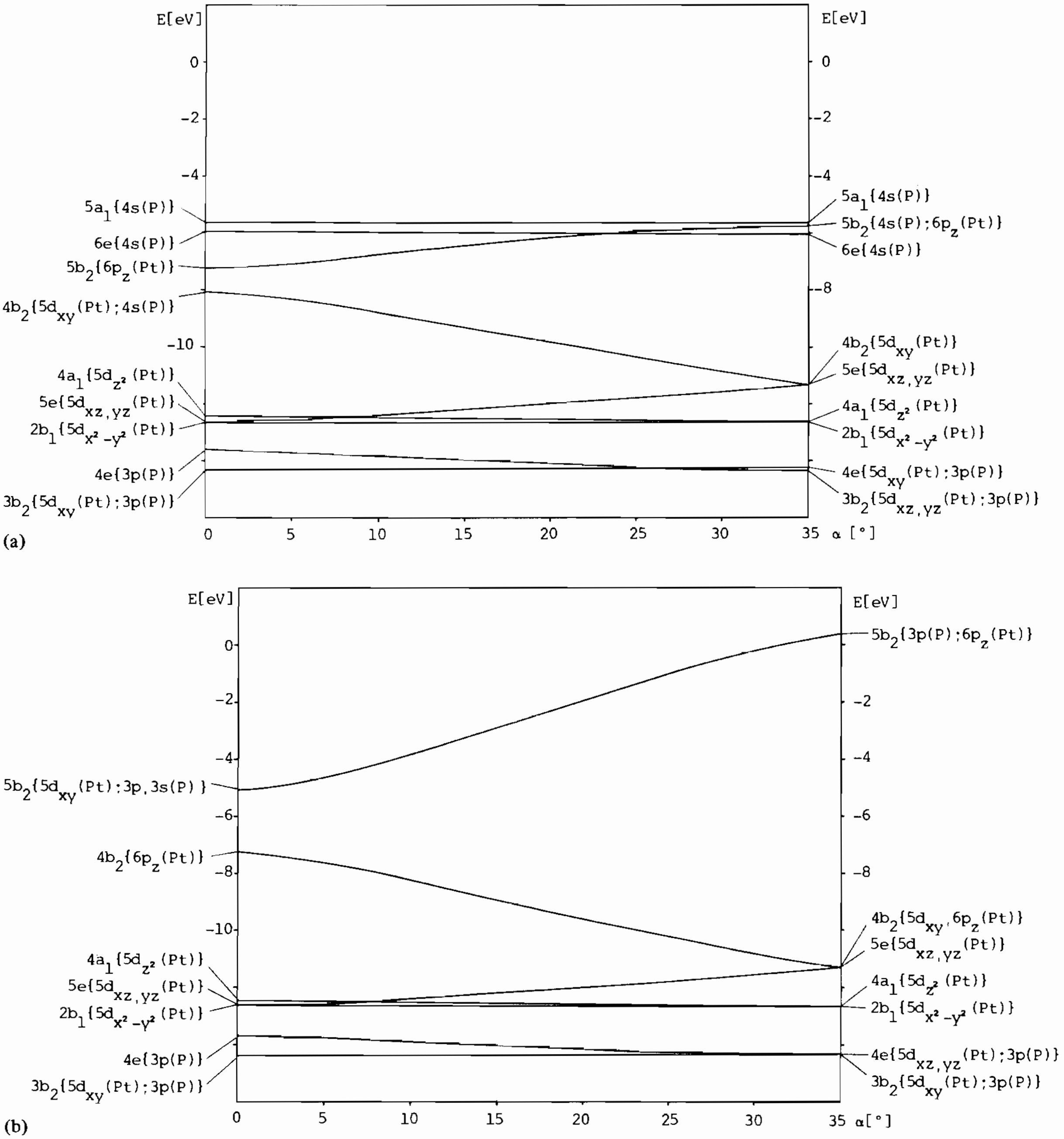

Fig. 5. Calculated one-electron energies for $[Pt(PH_3)_4]^{2+}$ as a function of molecular geometry. For the definition of α, see the text. The preponderant components of the MO's are given in parentheses. In Fig. 5(a), the following atomic orbitals were used in the calculations: Pt: 5d, 6s, 6p; P: 3s, 3p, 4s; H: 1s. In Fig. 5(b), 4s(P) orbitals have been omitted.

References

1 V. Gramlich, W. Petter and J. Kozelka, unpublished results.

2 K. Jensen, *Z. Anorg. Allg. Chem.*, *229*, 225 (1936).

3 J. Kozelka and W. Ludwig, *Helv. Chim. Acta*, *66*, 902 (1983).

4 D. A. Dudell, P. L. Goggin, R. J. Goodfellow, M. G. Norton and J. G. Smith, *J. Chem. Soc. (A)*, 545 (1970).

5 P. S. Pregosin and R. W. Kunz, '^{31}P and ^{13}C NMR of Transition Metal Phosphine Complexes', NMR-Basic Principles and Progress, Vol. 16, Springer, Berlin, 1979.

6 P. L. Goggin, R. J. Goodfellow, J. R. Knight, M. G. Norton and B. F. Taylor, *J. Chem. Soc., Dalton*, 2220 (1973).

TABLE VIII. Calculated Oscillator Strengths for Planar ($\alpha = 0°$) and Tetrahedrally Distorted ($\alpha = 15°$) $[Pt(PH_3)_4]^{2+}$.

	Preponderant character	Transition	Oscillator strength $\alpha = 0°$	$\alpha = 15°$
Valence-Shell Transitions	Ligand-field transitions	$5e \rightarrow 4b_2$	0.0004	7.10^{-5}
		$2b_1 \rightarrow 4b_2$	0.0	0.0
		$4a_1 \rightarrow 4b_2$	0.0002	0.032
	Ligand-to-metal charge transfer	$4e \rightarrow 4b_2$	0.578	0.421
Rydberg-Transitions	Metal-to-ligand charge transfers	$5e \rightarrow 6e$	0.002	0.024
		$2b_1 \rightarrow 6e$	0.065	0.051
		$4a_1 \rightarrow 6e$	0.006	0.004
		$5e \rightarrow 5a_1$	10^{-6}	0.034
		$2b_1 \rightarrow 5a_1$	0.0	0.0
		$4a_1 \rightarrow 5a_1$	0.0	0.0
	Transitions within the ligand system	$3b_2 \rightarrow 6e$	0.391	0.175
		$4e \rightarrow 6e$	0.003	0.069
		$3b_2 \rightarrow 5a_1$	2.10^{-5}	0.056
		$4e \rightarrow 5a_1$	0.459	0.387
	Platinum-internal d-p-transitions	$5e \rightarrow 5b_2$	0.267	0.242
		$2b_1 \rightarrow 5b_2$	0.0	0.0
		$4a_1 \rightarrow 5b_2$	0.352	0.242

TABLE IX. Spectral Parameters of Complexes $[Pt(PR_3)_4]X_2$. (Transition energies in cm^{-1}, ϵ-values $[M^{-1} \cdot cm^{-1}]$ in parentheses. s = shoulder.)

Complex	Solvent	Ligand-field-bands		Band 'A'		Band 'B'
$[Pt(PMe_3)_4]Cl_2$	H_2O		33900s (1400)	37300 (3750)	44200s (10100)	48500 (48200)
$[Pt(PEt_3)_4](ClO_4)_2$	H_2O	28600s (700)	32200s (2200)	35200 (4200)	42000s (9000)	45900 (44000)

7 H. Basch, A. Viste and H. B. Gray, *Theoret. Chim. Acta, 3*, 458 (1965).

8 R. Munita and J. R. Letelier, *Theoret. Chim. Acta, 58*, 167 (1981).

9 J. H. Ammeter, H. B. Bürgi, J. C. Thibeault and R. Hoffmann, *J. Am. Chem. Soc., 100*, 3686 (1978).

10 C. J. Ballhausen and H. B. Gray, *Inorg. Chem., 1*, 111 (1962).

11 E. Clementi and C. Roetti, *Atomic Data and Nuclear Data Tables, 14*, 177 (1974).

12 H. Basch and H. B. Gray, *Theoret. Chim. Acta, 4*, 367 (1966).

13 W. W. Meyer, Dissertation, Universität Zürich, Zürich, 1981.

14 G. G. Messmer and E. L. Amma, *Inorg. Chem., 5*, 1775 (1966).

15 G. R. Clark, B. W. Skelton and T. N. Waters, *J. Organomet. Chem., 85*, 375 (1975).

16 R. A. Jones, F. Mayor Real, G. Wilkinson, A. M. R. Galas, M. B. Hursthouse and K. M. A. Malik, *J. Chem. Soc., Dalton*, 511 (1980).

17 Landolt-Börnstein, Numerical Data and Functional Relationships in Science and Technology, New Series, Vol. II/7, 90.